

## RF Dipole Coil backed by a High-Impedance-Surface Shield

Zhichao Chen<sup>(1)</sup>, Andreas Rennings<sup>(1)</sup>, Klaus Solbach<sup>(2)</sup>, and Daniel Erni<sup>(1)</sup>

<sup>(1)</sup>Laboratory for General and Theoretical Electrical Engineering (ATE)  
Faculty of Engineering, University of Duisburg-Essen, D-47048 Duisburg, Germany

<sup>(2)</sup>Laboratory for High Frequency Engineering (HFT)  
Faculty of Engineering, University of Duisburg-Essen, D-47048 Duisburg, Germany

E-Mail: [zhi.chen@uni-due.de](mailto:zhi.chen@uni-due.de)

Web: <http://www.ate.uni-due.de/index.htm>

**Abstract** – In this contribution we present a novel approach to enhance the  $B_1$  distribution of a RF dipole coil by utilizing a high-impedance-surface (HIS) shield for ultra-high field (UHF) magnetic resonance imaging (MRI).

The simulation model for the investigation of improving the  $B_1$  homogeneity with a HIS shield is displayed in Fig. 1. A 25 cm-long symmetrically fed dipole element, which is terminated by two meanders has been employed as an excitation of the  $B_1$  field. The geometry of the meander remains unchanged in comparison to [2]. In order to fine-tune the current distribution on the strip line, high-dielectric substrates ( $\epsilon_r=11.2$ ) have been placed around the meander sections [3]. A two-dimensional HIS (EBG) structure [3] which operates as the RF shield is located below the dipole element with a separation distance of  $d$ . Additionally to the HIS case, two other shielding scenarios are considered here for the purpose of comparison: a perfect electric conductor (PEC), which models the conventional metallic shielding plate, and a perfect magnetic conductor (PMC), which exhibits an absolute surface current suppression (ideal case for a HIS shield).

In order to model the human body at 300 MHz, a homogenous flat phantom ( $\epsilon_r=58.2$ ,  $\sigma=0.92$  S/m) is placed 2 cm above the dipole element.

The  $B_1$  field distributions in the transverse cut-plane of the phantom (cf. Fig. 1) for different shielding scenarios (PEC, HIS and PMC) are shown in Fig. 2. The corresponding field distribution is normalized to the square root of the peak SAR inside the phantom. The effect of a variation of the separation distance from the dipole coil to the RF shields ( $d = 5$  mm, 10 mm, 20 mm) is investigated here. In general, the HIS shield behaves quite similar to the PMC condition and provides an improved  $B_1$  homogeneity due to the broader field distribution in comparison to the PEC condition (cf. Fig. 2). For a small separation distance, the HIS has an advantage over the PEC shield considering the magnetic field distribution inside the phantom. Since the induced current on the PEC shield considerably affects the  $B_1$  field excited by the dipole coil due to proximity, whereas the surface current on the HIS shield is sufficiently suppressed. For an increased separation distance, the impact of the induced current is weakened and, thus, changes on the field distribution with different shielding scenarios (HIS and PEC) are reduced. Additionally, the penetration depth is slightly enhanced by utilizing a HIS/PMC shield, indicating by the extended equipotential lines of the  $B_1$  distribution (cf. Fig. 2).

Fig. 3 shows the measured transverse magnetic field distribution for different shielding plate: a copper-plated substrate and a two-dimensional HIS structure [4]. The separation distance between the dipole and the corresponding shielding plate is set to 1 cm. Similar to the simulation, the magnetic

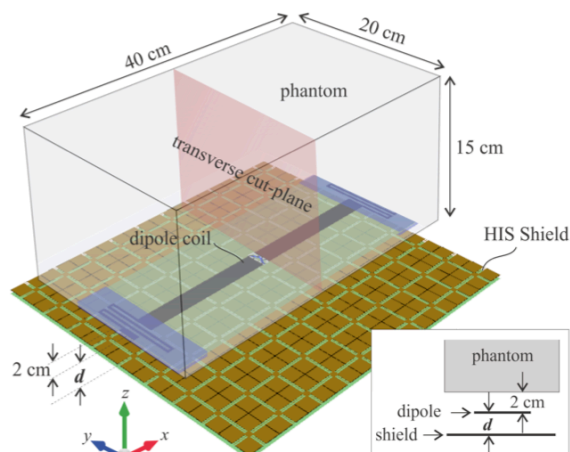


Fig.1: The simulation model in EMPIRE XPU for the investigation of improving the  $B_1$  homogeneity with a HIS shield and the effect of different separation distance from the dipole coil to the shielding plate [1].

field is normalized to the square root of peak SAR inside the phantom and plotted in dB. The measurement results in Fig. 3 indicate that a broader magnetic field distribution in transversal direction can be achieved by using a HIS shield compared to the conventional metal shield. Additionally, the absolute penetration of the magnetic field inside the phantom is slightly improved as well. The multi-channel coil arrangement is currently under investigation.

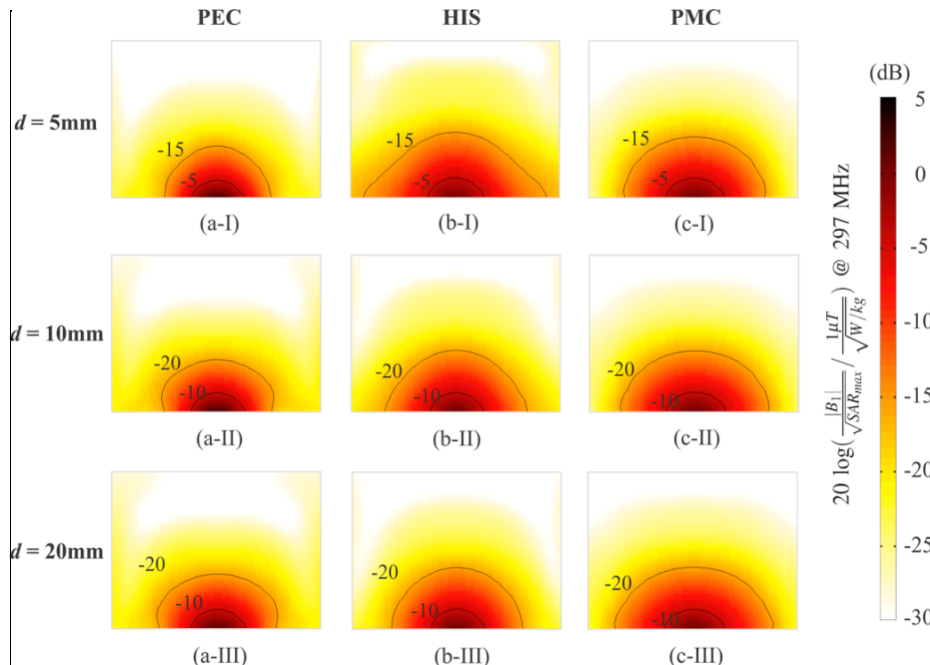


Fig.2: Simulated transverse  $|B_1|$  field distribution of the dipole coil inside the phantom for different shielding plates (PEC (a), HIS (b) and PMC (c)) and separation distances ( $d=5$  mm, 10 mm, 20 mm) at 300 MHz. The corresponding field distribution is normalized to the square root of the peak SAR and plotted in dB [1].

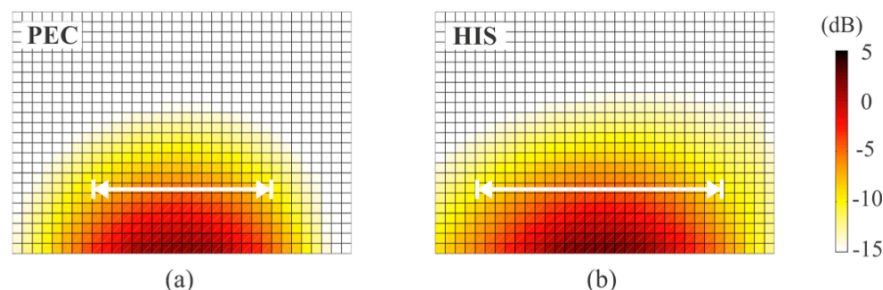


Fig.3: Measured transverse  $|B_1|$  field distributions at 300 MHz for different shielding plates: a copper-plated substrate (a) and a two-dimensional EBG structure (b). The corresponding  $|B_1|$  fields (in  $\mu\text{T}$ ) are normalized to the square root of peak SAR inside the phantom and plotted in dB [5].

## References

- [1] Z. Chen, K. Solbach, D. Erni, and A. Rennings, "Improved B1 Homogeneity of an MRI RF Coil Element using a High-Impedance-Surface Shield," in *9th German Microwave Conference (GeMiC 2015)*, March 16-18, Nürnberg, Germany, pp. 111-114, 2015.
- [2] S. Orzada, A. Bahr, and T. Bolz, "A novel 7 T microstrip element using meanders to enhance decoupling," in *16th Proc. Intl. Soc. MRM*, p. 2979, 2008.
- [3] Z. Chen, K. Solbach, D. Erni, and A. Rennings, "Dipole RF Element for 7 Tesla magnetic resonance imaging with minimized SAR," in *7th European Conference on Antennas and Propagation (EuCAP 2013)*, April 8-12, Gothenburg, Sweden, pp. 1716-1719, 2013.
- [4] Z. Chen, K. Solbach, D. Erni, and A. Rennings, "A Compact Electromagnetic Bandgap Structure based on Multi-layer Technology for 7-Tesla Magnetic Resonance Imaging Applications," in *44th European Microwave Conference (EuMC 2014)*, Oct. 6-9, Rome, Italy, pp. 1576-1579, 2014.
- [5] Z. Chen, K. Solbach, D. Erni, and A. Rennings, "Electromagnetic Field Analysis of a Dipole Coil Element with Surface Impedance Characterized Shielding Plate for 7-Tesla MRI," *IEEE Trans. Microw. Theory Techn.*, doi: 10.1109/TMTT.2016.2518168, Januar 2016.